ELSEVIER

Journal of Nuclear Materials 266–269 (1999) 343–347

journal of nuclear materials

New results on carbon release and transport in ASDEX-Upgrade

A. Kallenbach [a,*], A. Bard [a], D. Coster [a], R. Dux [a], C. Fuchs [a], J. Gafert [b], A. Herrmann [a], R. Schneider [a], ASDEX-Upgrade Team

[a] *Max-Planck-Institut für Plasmaphysik, IPP–EURATOM Association, D-85748 Garching, Germany*
[b] *Institut f. Plasmaforschung, Universität Stuttgart, D-70569 Stuttgart, Germany*

Abstract

The behaviour of carbon in the divertor of ASDEX-Upgrade is investigated by means of optical spectroscopy, bolometry and thermography. Apparent chemical erosion yields, derived from CH molecular band emission and H_β spectroscopy are shown to exhibit a pronounced flux dependence and isotope effect, $Y_{\text{chem}} \propto m_{\text{H}} \times \Gamma^{-0.7}$, while no dependence on surface temperature ($T_{\text{surf}} < 100°\text{C}$) and impact energy is seen. The flux and isotope dependences also show up in the CII, CIII and total carbon radiation. The weak correlation between the carbon yields in the divertor and the core plasma carbon concentration supports the assumption that main chamber sources are important for the core plasma carbon content under the low temperature, high recycling conditions of this study. © 1999 Elsevier Science B.V. All rights reserved.

Keywords: Carbon; Chemical erosion

1. Introduction

Chemical erosion and transport of carbon are important processes for the appropriate choice of plasma facing components in a future fusion device like ITER. Of particular interest is their impact on component lifetime, tritium codeposition and the role of carbon radiation in the achievement of low power densities at the target plate [1,2]. In a recent paper [3], evidence for a pronounced reduction of the apparent chemical erosion yield with increasing hydrogen flux was reported, which has been obtained from CH band and H_β spectroscopy. However, the observed reduction of the intensity ratios of the molecular band and the H_β line with hydrogen flux Γ_{H} could not unambiguously be interpreted as the corresponding reduction of the chemical erosion yield Y_{chem} with flux. The reasons are uncertainties in the atomic data and divertor plasma parameters necessary for the evaluation of the yields and cross-correlations of plasma parameters during the experimental parameter variations. In particular, the possible flux and energy dependences could not be disentangled due to a strong experimental correlation of the impact energy E and $1/\Gamma_{\text{H}}$. There is evidence for an energy dependence of the chemical erosion yield in laboratory experiments [4], but the high flux densities typical of a tokamak divertor cannot be achieved by beam experiments, and extrapolation is uncertain unless all intermediate steps in hydrocarbon formation are understood in a quantitative way.

In this study, the parameter range for deuterium discharges could be considerably widened due to high power operation with 20 MW neutral beam heating now available at ASDEX-Upgrade, and the (experimental) correlation of particle flux and mean energy could be better resolved. In the following, the term ‘H’ is used for hydrogen and deuterium generically, ‘D’ refers to deuterium in particular. All data points shown are taken along the viewing line indicated in Fig. 1, the symbol coding explained in Fig. 2 is used throughout this paper.

---

[*] Corresponding author. Tel.: +49 89 3299 1721; fax: +49 89 3299 1812; e-mail: kallenbach@ipp.mpg.de.

PII: S0022-3115(98)00666-7

2. Derivation of erosion yields

Chemical erosion yields are determined by spectroscopic measurements of CH molecular band emission [5] and H_β line intensities in the outer divertor of ASDEX Upgrade. Fig. 1 shows the experimental arrangement and typical experimental profiles along the target for the power load, ion saturation current, CIII (465 nm) and D_β emission. In addition, the variation of electron density n_e and temperature T_e along the viewing line is indicated taken from B2-EIRENE modelling of a typical attached, high power case. The target material is carbon fibre composite (CFC). In the following, we consider only experimental conditions which are attached around the crossing point of the line of sight with the target.

The spatial D_β and CIII profiles in Fig. 1 are measured by a multichordal [6] photomultiplier system equipped with interference filters. To determine erosion yields a spectrometer must be used because the CD band intensity is weak. The corresponding line of sight indicated in Fig. 1 is connected to a low-resolution mini-spectrometer PC-card equipped with a Si-photodiode array detector (Control Development Instruments). All data points represent the temporal average over at least 100 ms in order to reduce the statistical scatter and to average over several ELMs during H-mode.

There are three reasons for selecting the line of sight about 10 cm above the strike point: First, enough plasma line density must be present to allow for the ionization which is necessary for a spectroscopic particle flux measurement. Second, gradient lengths perpendicular to the viewing line must be longer than the mean free paths. The most important point is the contribution of recombination to the H_β line emission, which makes the interpretation of photon fluxes in terms of particle fluxes impossible. The corresponding high density, low temperature conditions appear first near the strike point and furthermore extend upward in the course of developing detachment. The contribution of recombination to the hydrogen lines is seen around $s = 1.10$ m in Fig. 1, where the population of higher lying hydrogen states by recombination contributes to the measured H_β emission. This contribution is experimentally detected by the line ratio drop of H_β/H_γ.

The atomic physical factor used to evaluate the hydrogen flux is the ratio *S*/XB of ionization and photon emission probabilities, the corresponding quantity *D*/XB used for the molecular flux refers to the number of dissociations taking place per emitted photon. By multiplying *S*/XB and *D*/XB with the measured atomic and molecular photon flux densities the particle flux densities are obtained, provided that all particles are ionized or dissociated along the line of sight and electron impact is the mechanism of spectral line excitation. Spectroscopic Γ_H measurements are no longer possible when recombination dominates the H_β emission. Such conditions routinely apply for the inner divertor, where detachment is more easily achieved; the corresponding plasma parameters are $T_e \approx 1$ eV and n_e up to 10^{21} m^{-3} [7].

The chemical erosion yield in the upper outer divertor is calculated from the absolutely calibrated measurements via

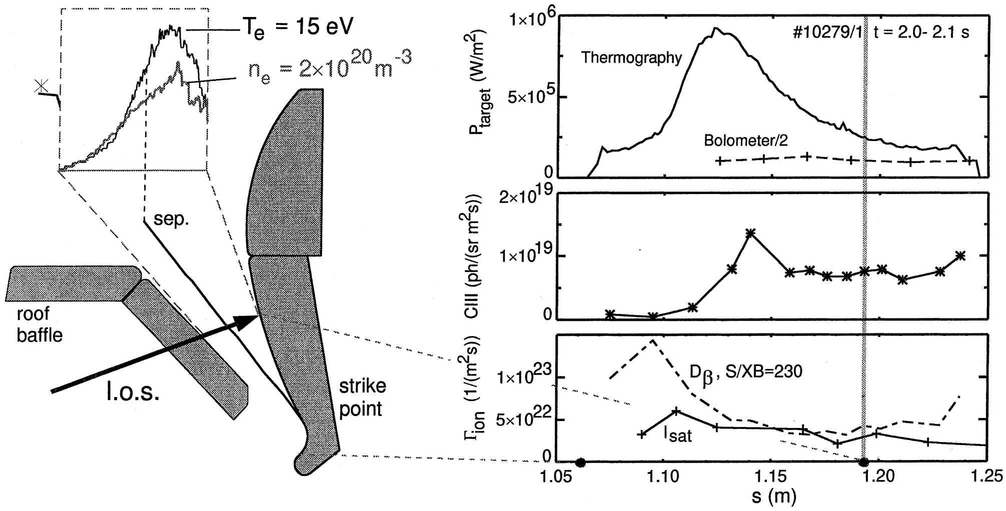

Fig. 1. Left: Experimental arrangement for the line of sight (l.o.s.) used for spectroscopic particle flux measurements in the outer divertor (Div-II) of ASDEX Upgrade. Typical profiles of n_e and T_e along the l.o.s. from B2-EIRENE modelling are also shown. Right: Profiles of total power load (thermography), radiative power load (bolometry), CIII emission (visible spectroscopy array with interference filters, IF) and particle fluxes from Langmuir probes and D_β spectroscopy (IF) for an H-mode discharge with $P_{heat} = 8$ MW.

$$Y_{\mathrm{chem}} = \Gamma_{\mathrm{CH_4}}/\Gamma_{\mathrm{H}} = \frac{D/\mathrm{XB}(\mathrm{CH_4})}{S/\mathrm{XB}(\mathrm{H_\beta})} \times \frac{I(\mathrm{CH})}{I(\mathrm{H_\beta})}. \tag{1}$$

In the following, we use $S/\mathrm{XB} = \mathrm{const} = 230$ for the $\mathrm{H_\beta}$ line. The 'effective' value $D/\mathrm{XB} = \mathrm{const} = 50$ is used to extrapolate the total hydrocarbon flux from the (actually measured) CH flux using a simple model for the loss of intermediate neutral and ionized molecular breakup products [5]. First results of a Monte Carlo calculation with the ERO code and a discussion of the T_e and n_e dependences of D/XB can be found in Ref. [8]. Besides $\mathrm{CH_4}$, heavier hydrocarbons are expected to be eroded with fluxes comparable to those of methane. These heavier hydrocarbons are covered by our measurement only via the CH molecules originating from their breakup. Realistic calculations of their breakup chain are not available so far. Assuming that a lower fraction of the carbon atoms bound in $\mathrm{C}_x\mathrm{H}_y$ molecules ends up as CH in comparison to $\mathrm{CH_4}$, the total hydrocarbon yield calculated by our effective D/XB represents the lower limit. Therefore, the parameter dependence of our effective D/XB is the major source of uncertainty (factor 2) for the experimental chemical erosion yields.

Numerical parameter studies have shown that taking a constant S/XB for $\mathrm{H_\beta}$ is a fair approximation of the experimental situation, since the parameter variations of S/XB on n_e and T_e tend to partly cancel in the experiment. Typical values for T_e measured by Langmuir probes at the plate are 5–15 eV, the electron densities vary $1\text{–}5 \times 10^{19}\ \mathrm{m^{-3}}$, higher temperatures corresponding to lower densities. The lowest values of the density are not relevant for the evaluation of S/XB, since the long mean free path of the particles causes a penetration deeper inside the divertor plasma, where higher densities exist. The approximation of $S/\mathrm{XB} = \mathrm{const}$ is also confirmed by the fact that spectroscopic hydrogen fluxes agree with the ion fluxes obtained from the Langmuir probes within a factor of 2. The hydrogen ion flux profiles along the outer target shown in Fig. 1 demonstrate a typical situation. The $\mathrm{H_\beta}$ line intensities measured along identical viewing lines in different toroidal positions with the minispectrometer and the interference filter/multiplier system agree within 20%, which corresponds to the uncertainties of the individual calibrations. The error of the CH band intensities is slightly higher ≈30% due to the line fitting procedure and the influence of spurious lines.

3. Regression analysis

The experimental parameters which presumably have an impact on the chemical erosion yield are the flux Γ_{H}, the hydrogen impact energy E, the atomic mass of the incident hydrogen ions and atoms m_{H} and the target surface temperature T_{surf}. Since no direct measurement for the impact energy E is available, we estimate E from the particle flux density Γ_{H} and the power density P_{target} from thermography, which has to be corrected for the contribution of radiation. The latter is approximated by half the measured line integral $P^{\mathrm{bolo}}_{\mathrm{line}}$ ($\mathrm{W/m^2}$) on the corresponding line of sight (l.o.s.) (see Fig. 1), according to a simulation based on reconstructed emission profiles. The impact energy E is approximated via

$$E = (P_{\mathrm{target}} - P^{\mathrm{bolo}}_{\mathrm{line}}/2 - \Gamma_{\mathrm{H}} \times E_{\mathrm{ion}})/\Gamma_{\mathrm{H}} \times \gamma_{\mathrm{i}}/\gamma, \tag{2}$$

where γ and γ_{i} represent the total and the ion sheath transmission factors and E_{ion} is the hydrogen ionization potential released during recombination at the surface. We use $\gamma = 8$ and $\gamma_{\mathrm{i}} = 4$, assuming that half of the energy is carried by hydrogen ions. This averaged value for E does not take into account the energy distribution of the ions, the molecular dissociation energy and the contribution of low-energy neutrals which are produced by charge-exchange collisions or $\mathrm{H_2}$ breakup close to the wall.

No significant dependence of Y_{chem} on the surface temperature is found in a multiparameter regression. Regression analysis of the obtained yields versus energy E, mass m_{H} and flux Γ_{H} for fluxes $\Gamma_{\mathrm{H}} > 10^{22}\ \mathrm{m^{-2}\ s^{-1}}$ results in

$$Y_{\mathrm{chem}}(\%) = 0.92 \times \Gamma_{\mathrm{H}}^{-0.68} \times E^{0.07} \times m_{\mathrm{H}}^{1.03} \quad (10^{22}\ m^{-2}\ \mathrm{s^{-1}}, \mathrm{eV}, \mathrm{amu}). \tag{3}$$

Very similar results are obtained when the ion saturation current is used to calculate Γ_{H} and E. Since the energy dependence in Eq. (3) is not significant within the experimental uncertainties, and the isotope effect is almost proportional to the mass, we used the fixed ansatz $Y_{\mathrm{chem}} \propto m_{\mathrm{H}} \times E^0$ for the regression of Y_{chem} versus Γ_{H} for fluxes $\Gamma_{\mathrm{H}} > 10^{22}\ \mathrm{m^{-2}\ s^{-1}}$:

$$Y_{\mathrm{chem}}(\%) = 1.18 \times m_{\mathrm{H}} \times \Gamma_{\mathrm{H}}^{-0.7} \quad (\mathrm{amu}, 10^{22}\ m^{-2}\ \mathrm{s^{-1}}). \tag{4}$$

Fig. 2 shows the measured erosion yields versus flux Γ_{H}. The scaling for H and D as predicted by Eq. (4) is drawn as slanted lines, the horizontal dashed lines indicate typical (flux-independent) results from laboratory experiments obtained under low-flux conditions.

As already noted, the regression analysis of the experimental yields shows no significant dependence (exponents less than 0.1 in power law description) on target temperature and impact energy. To visualize this finding, Fig. 3 displays the measured yields divided by yields according to Eq. (4) versus: (a) the target temperature obtained from thermography and (b) the impact energy estimated from power load corrected by bolometry. In Fig. 3, Eq. (4) is evaluated for hydrogen to better separate the D and H data and to underline the isotope effect.

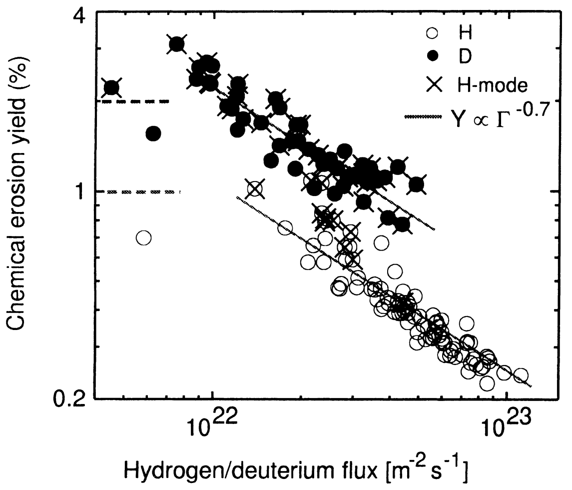

Fig. 2. Chemical erosion yields, derived from CH/CD molecular band emission versus hydrogen/deuterium flux densities for various experimental conditions in hydrogen and deuterium plasmas in ASDEX Upgrade Div-II.

4. Impact of carbon erosion on divertor radiation and core carbon content

The carbon production in the divertor is important for the radiative power removal below the x-point and therefore an ingredient for the observed low peak power densities at the plate (see Fig. 1 or Ref. [1]). The isotope effect seen in the chemical erosion yields for carbon (note there is also an isotope effect in the corresponding physical sputtering yields, depending on the impact energy) also shows up in the CII and CIII line intensities ($Y_{\mathrm{CII,CIII}} \propto \Gamma^{-1}$, see Fig. 4(a)) and in the radiated power measured by bolometry. Fig. 4(b) shows the total hydrogen radiation and the sum of CII and CIII radiation normalized to the line-integrated radiation measured by the corresponding bolometer chord. The total hydrogen radiation is projected from the H_β emission, the total CII and CIII radiation is projected from individual lines under the assumption $T_{\mathrm{e}}^{\mathrm{emission}} = E^{\mathrm{ion}}/3$ using the ADAS atomic data base. For low hydrogen fluxes, carbon radiation dominates, while at high fluxes the hydrogen radiation prevails. The reconstructed ‘spectroscopic’ radiation typically accounts for 50% of the bolometric value. This degree of agreement is satisfactory, taking into account uncertainties in atomic data and plasma parameters and the fact that the radiation from boron, CI and CIV is omitted. Generally, hydrogen radiation is more important in hydrogen plasmas in comparison to deuterium plasmas due to the isotope effect in the carbon erosion.

It is worthwhile to compare the erosion yield with the carbon concentration in the main plasma, although the latter is believed to be only weakly coupled to the erosion rates deep in the divertor in the medium-to-high density operational region of ASDEX Upgrade. In fact no correlation is visible between the divertor chemical yields and the core carbon concentrations (the same picture is obtained when the CIII yield is used). Evidence for the importance of main chamber sources for the core carbon content had been reported earlier [9]. An additional hint is the fact that the typical carbon concentrations in the main plasma are virtually the same (0.5–1.5% in deuterium) in the present Div-II and in the tungsten-coated Div-I. The isotope effect for the net carbon erosion, which is also present at low flux densities also shows up in the main plasma carbon content.

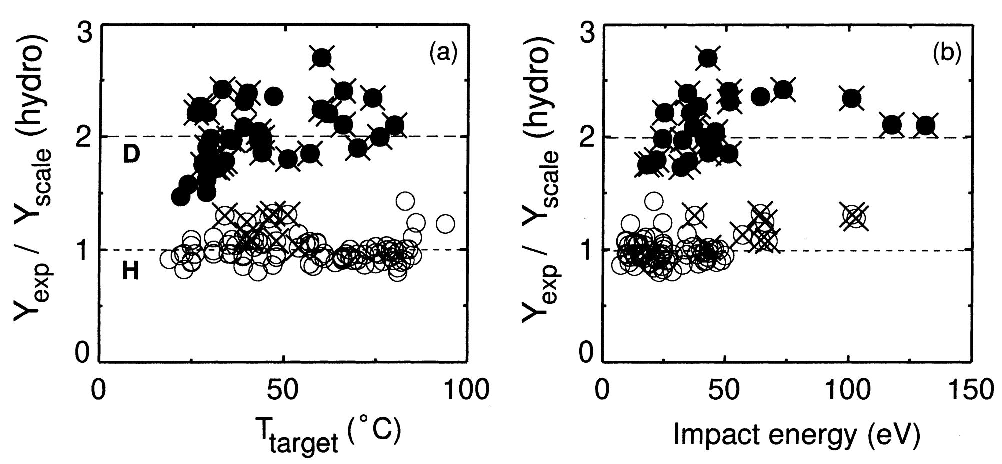

Fig. 3. Measured erosion yields, normalized by the scaling Eq. (4) evaluated for hydrogen, (a) versus target surface temperature and (b) versus impact energy calculated from radiation-corrected deposited power.

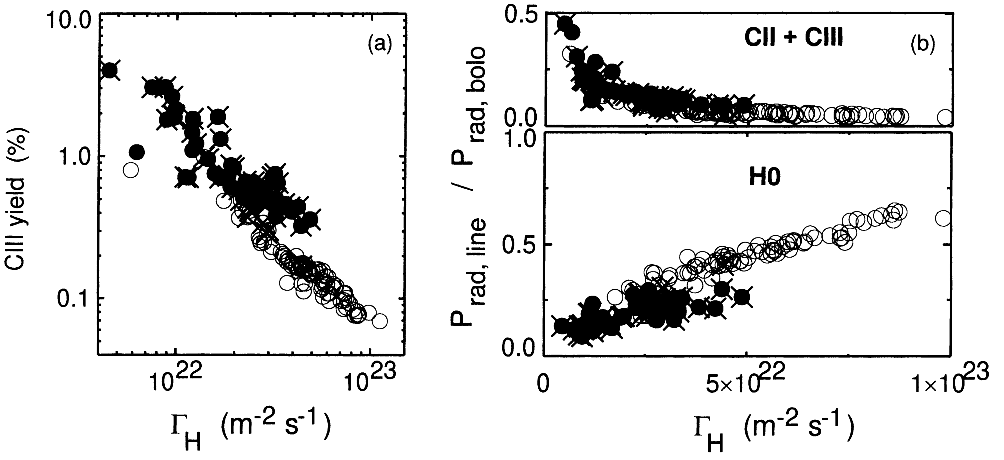

Fig. 4. (a) Total C^{2+} erosion yield, obtained from CIII emission. (b) Line integrated radiation, reconstructed from individual lines of the corresponding species, normalized by bolometer measurements versus flux density.

5. Discussion

If Eq. (4) represents in fact a good empirical description of Y_{chem}, the question about the underlying physical mechanisms arises. At first sight, the primary candidate would be the kinetic ejection of surface hydrocarbon complexes due to collisional energy transfer, a process called Y_{surf} in [10]. The flux dependence would then be caused by the fact that this collisional process does no longer determine the erosion rate. But, the isotope effect should vanish or weaken under these conditions, since the better momentum transfer to hydrocarbons by deuterium can no longer lead to correspondingly higher erosion rates when the erosion rate has become independent of the collision frequency. The isotope effect shown in Fig. 2 does not exhibit a reduction at higher fluxes. Therefore, the process Y_{surf} should not be considered responsible for the observed behaviour of the apparent Y_{chem}. This is more probably caused by an intermediate step in the hydrocarbon formation. More work is necessary to reduce the uncertainties in the measurement of Y_{chem} and to identify possible reaction steps which explain the behaviour expressed by Eq. (4).

The major source of uncertainty in the interpretation of the obtained spectroscopic yields is the possibility of a fast, flux-dependent redeposition of molecular products before the photon emission takes place. This – hypothetic – effect is not taken into account by the *D*/XB used for the evaluation. Such a fast redeposition due to plasma interaction would not be seen in laboratory beam experiments measuring the chemical erosion yield. However, such a fast redeposition would have a similar positive effect on target lifetime as a direct, flux-dependent reduction of the underlying chemical processes.

References

[1] A. Herrmann, C. Fuchs, P. Franzen, V. Rohde, M. Weinlich et al., these Proceedings.
[2] R. Schneider et al., these Proceedings.
[3] A. Kallenbach, A. Thoma, A. Bard, K. Behringer, K. Schmidtmann, M. Weinlich, ASDEX Upgrade Team, Nucl. Fusion 38 (7) (1998) 1097.
[4] B. Mech, A. Haasz, J. Davis, J. Nucl. Mater. 241–243 (1997) 1147.
[5] K. Behringer, J. Nucl. Mater. 176&177 (1990) 606.
[6] J. Gafert, D. Coster, C. Dorn, B. Napiontek, U. Schumacher et al., Europhysics Conference Abstracts, in: M. Schittenhelm, R. Bartiromo, F. Wagner (Eds.), Proceedings of the 24th EPS Conference on Controlled Fusion and Plasma Physics, Berchtesgaden, vol. 21A, part IV, Petit-Lancy, EPS, 1997, pp. 1397–1400.
[7] U. Wenzel et al., these Proceedings.
[8] D. Naujoks, D. Coster, H. Kastelewicz, R. Schneider, these Proceedings.
[9] A. Kallenbach, R. Neu, W. Poschenrieder, The ASDEX Upgrade Team, Nucl. Fusion 34 (1994) 1557.
[10] J. Roth, C. García-Rosales, Nucl. Fusion 36 (1996) 1647.